Journal of Fluids and Structures (1997) **11,** 207–222

APPLICATION OF A GENERAL PURPOSE FINITE ELEMENT METHOD TO ELASTIC PIPES CONVEYING FLUID

L. G. OLSON AND D. JAMISON
Department of Mechanical Engineering, University of Nebraska–Lincoln
Lincoln, NE 68588-0656, U.S.A.

(Received 18 March 1996 and in revised form 26 November 1996)

The motion of elastic pipes conveying fluids has been studied extensively for various idealized cases for many years. In this paper we show that recent advances in finite element methodology have made it possible to simulate these coupled fluid–structure systems within the context of a general-purpose finite element program. Using a nonlinear Lagrangian–Eulerian finite element formulation we compare computational and theoretical results for four test cases with analytical solutions: a simplified cantilever pipe, a fixed–fixed pipe (clamped at both ends), a cantilever pipe, and a spring-supported cantilever pipe. Although care must be taken to match the finite element and theoretical modeling assumptions properly in all cases, the results show good agreement.

1. INTRODUCTION

AN ACCURATE UNDERSTANDING OF THE DYNAMICS of elastic pipes or tubes conveying fluids is necessary for engineering projects in many areas, including oil pipelines, nuclear reactor components, and marine drilling. The classic case of 'dynamics of elastic tubes conveying fluids' is the fire hose: as fluid flows rapidly through the flexible hose, the whipping motions of the hose can become quite violent. In general the tube will be stable up to some critical fluid flow velocity and will be unstable above this velocity.

Flexible tubes conveying fluids have been studied extensively both analytically and numerically. In most classic analyses the fluid is assumed to be inviscid and incompressible while the tube is linear elastic. The nature of the solutions is affected by the relative mass of the fluid and tube, by the flexibility and extensibility of the pipe, and very strongly by the boundary conditions on the tube. Calculating the critical flow velocities, mode shapes, and vibration frequencies can be a tedious task, although the governing equations themselves are quite elegant for simple geometries.

Recently, advances in finite element methodology have made it possible to simulate the dynamic motion of the fluid coupled with the flexible pipe for arbitrary geometries within the context of a general purpose finite element program. Figure 1 shows the classic problem of an elastic pipe conveying fluid whose behavior in the linear regime is well-established [see, for example, Chen (1987) or Païdoussis (1975)]. When there is no fluid in the pipe the resonant frequencies of the pipe (which then primarily acts as a beam) are easily calculated, and any general purpose commercial finite element code can perform the calculation for arbitrary geometries. If fluid is added to the pipe, but there is no flow, the resonant frequencies of the system are reduced by the added fluid mass. Most commercial finite element codes can handle this calculation, although care must be taken not to introduce spurious zero-energy modes due to the fluid (Olson &

0889–9746/97/020207 + 16 $25.00/fl960073

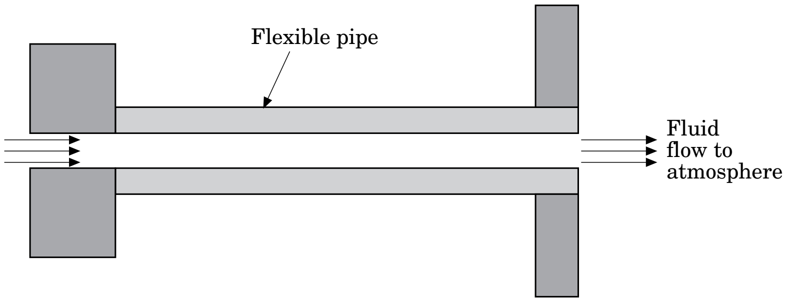

Figure 1. Typical geometry for elastic pipe conveying fluid.

Bathe 1983, 1985; Olson 1987). If the fluid is flowing through the pipe, the resonant frequencies of the system drop dramatically and even go to zero. It has only recently become possible to treat the coupled fluid flow and structural response with the advent of nonlinear Lagrangian–Eulerian finite element fluid-structure interaction formulations (Kock & Olson 1991; Nitikitpaiboon & Bathe 1993).

The response of elastic pipes conveying inviscid fluids has been studied extensively for various idealized cases since the 1950s, and the literature has been reviewed by Mote (1972), Wickert & Mote (1988), Chen (1987), Païdoussis (1987), and Païdoussis & Li (1993). Of particular interest to our work are the early studies of the now-classic cantilever and fixed–fixed (clamped at both ends) pipes. Benjamin (1961) and McIver (1973) investigated the application of Hamilton's Principle to an open system of changing mass, and McIver applied Hamilton's principle to flexible pipes conveying fluid by developing expressions for the potential and kinetic energies of the fluid and the pipe. Chen (1972a, 1973) studied the case of flow through curved tubes, and employed differential analyses and extended the application of Hamilton's Principle to these curved tubes and cylindrical structures. These investigations are particularly significant for our work, since the finite element formulation is based on a variational principle which must reduce to the appropriate governing equations. Païdoussis and his colleagues [see, for instance, Païdoussis (1970, 1975), Païdoussis & Sundararajan (1975), Hannoyer & Paidoussis (1979), Paidoussis, Cusumano & Copeland (1992)] have employed direct differential analysis to develop the governing equations and stability limits for pipes under a wide variety of flow and boundary conditions. Païdoussis' early work on flutter of conservative systems (Païdoussis 1975) was particularly useful in creating test cases for our finite element analysis. More recently, research has focused on the nonlinear dynamics of the systems under consideration [see the extensive review by Païdoussis & Li (1993)].

In a particular case involving nonlinear dynamics, Edelstein, Chen & Jendrzejczyk (1986) used a finite element method to solve the analytically derived equations for a cantilever pipe. They developed a time-dependent analysis to identify nonlinear beam behavior and limit cycles. While they employed Galerkin finite element methods which are similar to those we use, they developed a specific code to solve their specific problem.

By creating exact finite elements specifically for a broad class of pipe flow problems, Sällström (1990, 1993) and Sällström and Åkesson (1990) created a powerful numerical technique for solving the governing equations of pipe flow. The efficiency and accuracy of the technique is demonstrated on a number of test cases. Sällström's work is related to that of Edelstein *et al.* (1986) in that the general governing equations are first derived, and then finite element techniques are employed to solve them.

However, Sällström develops highly efficient exact finite elements, and Edelstein *et al.* employ higher order polynomial elements. In the general finite element formulation we employ in this paper, the geometries may be completely arbitrary, although the numerical calculations will be quite computationally intensive as a result.

Applications of general purpose finite element codes, with all their flexibility, has lagged substantially behind this theoretical and experimental work. In this study we shall verify that a general finite element formulation can (if applied judiciously) be used to predict accurately the transient response of flexible pipes conveying fluids by examining the results for four test cases with analytical solutions: a simplified cantilever pipe, a fixed–fixed pipe, a cantilever pipe, and a spring-supported cantilever pipe. We use the nonlinear $\mathbf{u}-\rho-\phi-\lambda$ fluid-structure formulation developed by Kock & Olson (1991) and implemented as an Arbitrary Lagrangian–Eulerian method by Nitikitpaiboon & Bathe (1993). (Although the commercial code ADINA includes this formulation, we employ the research code developed by Kock & Olson.) In this way we hope to demonstrate that finite element methods can be used to model specific pipe systems conveying fluids for arbitrary complicated geometries and boundary conditions of engineering interest.

2. MODELING ASSUMPTIONS

The assumptions generally used in creating models of flexible pipes conveying fluids are that (i) the pipe behaves as a single linear elastic beam with length L and properties E (Young's modulus), I (moment of inertia), and m (mass per unit length); (ii) the fluid moves in inviscid slug flow, with a constant uniform velocity U through the pipe; the fluid has a mass M per unit length and discharges to the atmosphere at the pipe outlet; (iii) the fluid–structure interface is such that the fluid moves with the pipe, and the pressure in the fluid acts on the pipe.

With these assumptions, the nondimensionalized governing equation for the simplest case becomes (Chen 1987)

$$\frac{\partial^4\eta}{\partial\xi^4}+u^2\frac{\partial^2\eta}{\partial\xi^2}+2\beta^{1/2}u\frac{\partial^2\eta}{\partial\xi\,\partial\tau}+\frac{\partial^2\eta}{\partial\tau^2}=0, \tag{1}$$

where $\beta=M/(M+m)$ is the relative mass of fluid, $u=U(ML^2/EI)^{1/2}$ is the relative flow speed of fluid, η is the dimensionless vertical displacement of the pipe, ξ is the dimensionless axial coordinate, and $\tau=[EI/(M+m)]^{1/2}t/L^2$ is the dimensionless time.

In order to allow direct comparisons to the analytical solutions, our finite element approach must include some restrictions as shown in Figure 2. The pipe is modeled as a standard 2-D nonlinear elastic solid (Bathe 1996), and the geometry is captured by using two plates with their neutral axes constrained to have equal vertical displacements. (This allows the fluid to be held between the plates, while the plates themselves

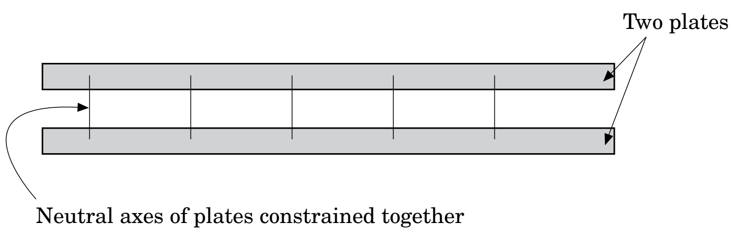

Figure 2. Finite element model for elastic pipe.

act as a single beam. While the constraint equations do not directly impose the condition that the solid act as a simple beam-like pipe, two long thin plates which are forced to move together in the vertical direction will naturally behave in this fashion.) The fluid itself is incompressible, inviscid, and irrotational, so that

$$\nabla^2 \phi = 0 \tag{2}$$

and

$$P_{\text{stag}} = P + \tfrac{1}{2}\rho(\nabla\phi)^2 + \rho\dot{\phi}. \tag{3}$$

Here ϕ is the velocity potential in the fluid, ρ is the fluid density, P is the pressure in the fluid, and P_{stag} is the stagnation pressure in the fluid. At the fluid–structure interface, the normal fluid velocity equals the normal solid velocity $\partial\phi/\partial n = \dot{u}_n$ and the fluid pressure, P, equals the normal stress in the solid.

The nonlinear finite element equations resulting from applying the assumptions discussed to the nonlinear $\mathbf{u} - \rho - \phi - \lambda$ formulation (Kock & Olson 1991) take the form

$$\begin{bmatrix} \mathbf{K}_{UU} + \mathbf{K}^{fs}_{UU} & (\mathbf{K}^{fs}_{\Phi U})^{\mathrm{T}} \\ \mathbf{K}^{fs}_{\phi U} & \mathbf{K}_{\Phi\Phi} \end{bmatrix} \begin{bmatrix} \mathbf{U} \\ \mathbf{\Phi} \end{bmatrix} + \begin{bmatrix} \mathbf{0} & (\mathbf{C}^{fs}_{\Phi U})^{\mathrm{T}} \\ -\mathbf{C}^{fs}_{\Phi U} & \mathbf{0} \end{bmatrix} \begin{bmatrix} \dot{\mathbf{U}} \\ \dot{\mathbf{\Phi}} \end{bmatrix} + \tag{4}$$

$$\begin{bmatrix} \mathbf{M}_{UU} & \mathbf{0} \\ \mathbf{0} & \mathbf{0} \end{bmatrix} \begin{bmatrix} \ddot{\mathbf{U}} \\ \ddot{\mathbf{\Phi}} \end{bmatrix} = \begin{bmatrix} \mathbf{R}_U \\ \mathbf{R}_\Phi \end{bmatrix} - \begin{bmatrix} \mathbf{F}_U \\ \mathbf{F}_\Phi \end{bmatrix}, \tag{5}$$

where $\mathbf{U}$ is the vector of nodal displacements for solid elements, $\mathbf{\Phi}$ is the vector of nodal velocity potentials for fluid elements, $\mathbf{R}_U$ represents the external loads on the structure, and $\mathbf{R}_\Phi$ is used to enforce inflow or outflow conditions on the fluid. $\mathbf{K}_{UU}$ is the stiffness matrix for the solid, $\mathbf{K}^{fs}_{UU}$ is a matrix incorporating stiffening of the solid caused by the fluid (if any), $\mathbf{K}^{fs}_{\Phi U}$ is the fluid–structure stiffness coupling, $\mathbf{K}_{\Phi\Phi}$ is a matrix to enforce fluid continuity, $\mathbf{C}^{fs}_{\Phi U}$ is a matrix to enforce fluid–structure boundary conditions, and $\mathbf{M}_{UU}$ is the mass matrix for the solid. A full description of the finite element formulation and the significance of each term is given in Kock & Olson (1991). ρ and λ, which normally appear as solution variables are not required since the fluid is incompressible and the mass of the fluid in the domain is allowed to vary if necessary.

Since this is a set of nonlinear time-dependent equations, we use them to find the transient response of the pipe–fluid system to an initial deflection and use that time response to identify characteristic frequencies by taking a Discrete Fourier Transform (DFT) of the time-dependent data. These characteristic frequencies can then be compared to the analytically predicted values. The analysis requires four steps:

(i) perform a linear frequency analysis with zero flow to identify the first mode of the pipe–fluid system with no flow;

(ii) fix the pipe in its first no-flow mode, and perform a nonlinear steady flow analysis; (this requires a full Newton iteration);

(iii) use the steady flow solution from (ii) as the initial condition for a nonlinear transient analysis; (this can be performed with a modified Newton iteration, using the original stiffness matrix throughout);

(iv) find characteristic frequencies by DFT analysis of the displacement *versus* time data for points on the pipe, if appropriate.

Note that this approach does not guarantee that we will identify the mode which will become unstable first, rather it simply analyses the transient response of the system to an initial condition which is very likely to excite at least a part of the mode which will become unstable first. In fact, several modes may be excited simultaneously.

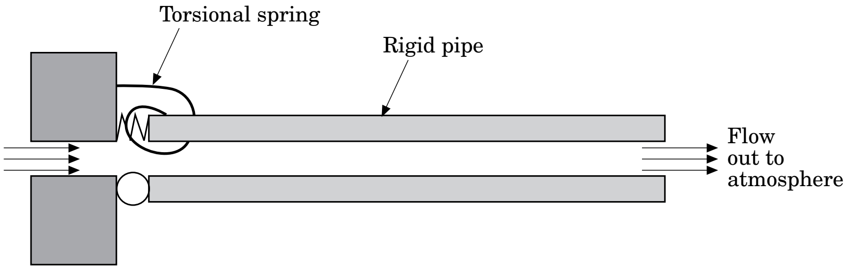

Figure 3. Simplified cantilever pipe test case.

3. TEST CASES

We demonstrate the procedure on four test cases. The first is a simplified cantilever pipe, which is a single degree-of-freedom system which nevertheless displays damping effects caused by fluid flow. The second is an idealized fixed–fixed pipe. The third case is a model of the cantilever pipe studied experimentally by Edelstein *et al.* (1986). The fourth test case is another cantilever pipe, this time clamped at the base and supported by a spring at the outflow end.

3.1. Simplified Cantilever Pipe

Figure 3 shows the simplified cantilever pipe test case. The pipe is modeled as rigid and all of the flexibility is lumped into the torsional spring k at its base. Applying conservation of energy to the system gives

$$\ddot{\alpha} + 2\zeta\omega_n\dot{\alpha} + \omega_n^2\alpha = 0, \tag{6}$$

where α is the angular deflection of the pipe,

$$\omega_n^2 = \frac{3k}{(M+m)L^3}, \tag{7}$$

and

$$\zeta = \frac{3UM}{2L\omega_n(M+m)}. \tag{8}$$

This has the usual solution for an initial angle α_0,

$$\alpha = \alpha_0 e^{-\omega_n\zeta t}\cos(\omega_n\sqrt{1-\zeta^2}t). \tag{9}$$

Notice that the fluid flow causes the mass-spring system to behave as a mass-spring-damper system, and that the damping depends on the fluid flow velocity.

Figure 4 shows the simple finite element model used for this test case, which contains only seven nodes. The pipe is arbitrarily chosen to be 10 m long and 1 m tall, and is made approximately rigid by setting its Young's modulus to $10^8\,\mathrm{N/m^2}$. The solid is taken as massless, while the fluid density is set at $1\,\mathrm{kg/m^2}$. The volume flowrate through the pipe is $Q = UA$, where A is $1\,\mathrm{m}^2$. The Young's modulus of the spring element is set so that the effective torsional stiffness is $k = 333\,\mathrm{N\,m}$. Overall, this gives a natural frequency ω_n of 1 rad/s and a damping ratio $\zeta = (3/20)U$. It is important to apply the inflow and outflow boundary conditions properly: at the inflow boundary we specify a zero velocity potential, while at the outflow boundary we impose that the gradient of the velocity potential is U. Figures 5 and 6 compare the analytical and

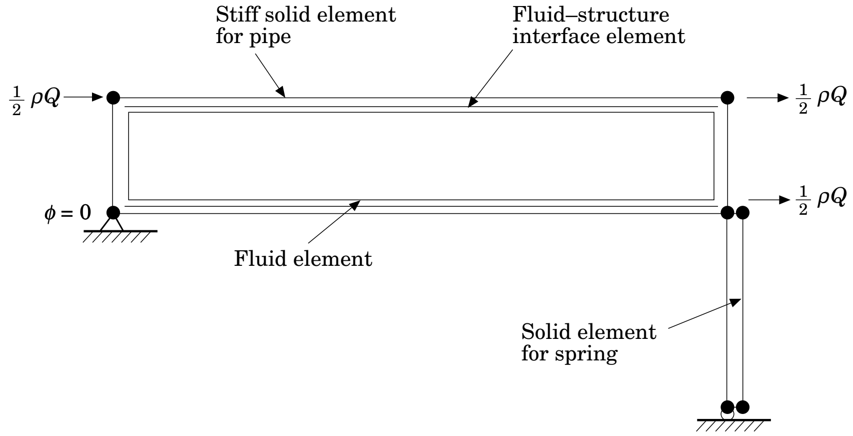

Figure 4. Finite element model for simplified cantilever pipe test case.

finite element results for tip deflection versus time for two flow speeds. We find good agreement between the two solution approaches.

3.2. Fixed-Fixed Pipe

Figure 1 shows the fixed–fixed pipe. For our analytical computation we choose the relative mass $\beta = 0{\cdot}1$ in equation (1) [following Païdoussis (1975)], and plot the dimensionless oscillation frequency versus dimensionless flow speed as shown in Figure 7. The oscillation frequency drops to zero as the flow speed increases, but there is no damping introduced for these conditions.

The two-dimensional finite element model for the problem is shown in Figure 8. The pipe consists of two plates, each 1 m $\times$ 0·01 m, with the vertical displacements of their

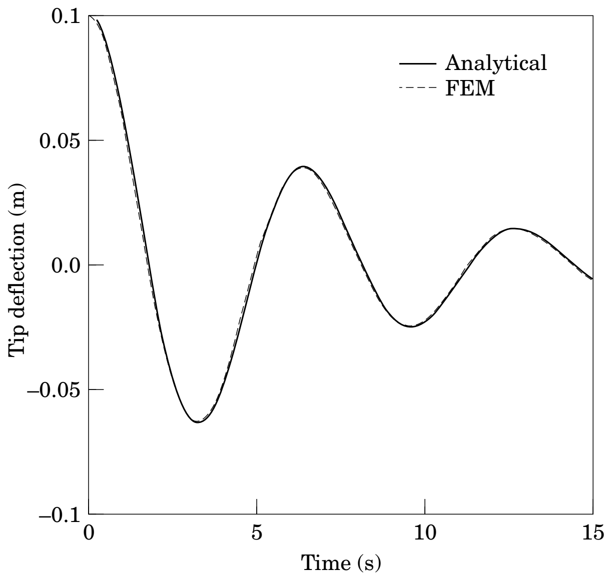

Figure 5. Comparison of finite element and analytical solutions to the simplified cantilever pipe test case; $U = 1$, $\zeta = 0{\cdot}15$.

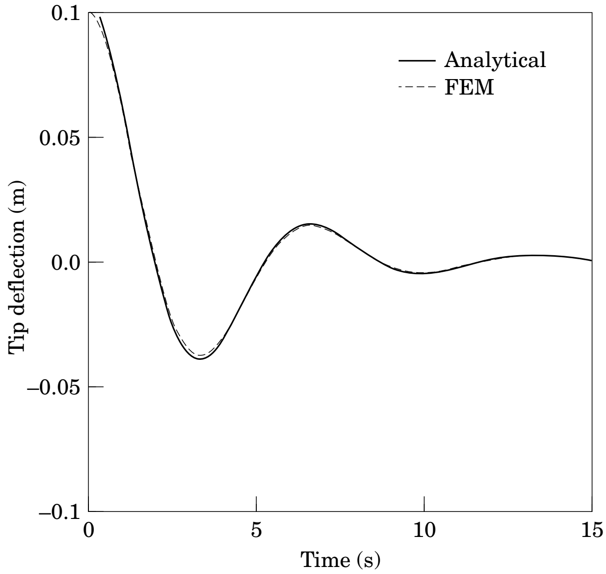

Figure 6. Comparison of finite element and analytical solutions to the simplified cantilever pipe test case; $U = 2$, $\zeta = 0{\cdot}3$.

neutral axes constrained together. Each plate is discretized with 300×2 four-node solid elements, with a Young's modulus of $1{\cdot}2 \times 10^9\,\mathrm{N/m^2}$, density of $9000\,\mathrm{kg/m^3}$, and a Poisson's ratio of zero. The fluid-filled gap between the plates is 0·02 m high and is discretized with 300×1 four-node fluid elements. The density of the fluid is taken to be $1000\,\mathrm{kg/m^3}$ so that the relative mass for the finite element model matches the $\beta = 0{\cdot}1$ for the analytical computation. Two-node fluid–structure interface elements line the "pipe" enforcing the compatibility between the fluid and solid elements. Here the

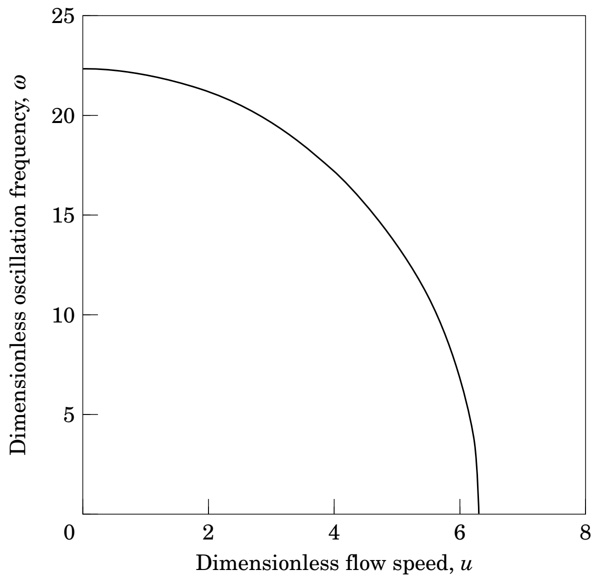

Figure 7. Dimensionless fundamental frequency versus dimensionless flow speed for fixed–fixed pipe with $\beta = 0{\cdot}1$.

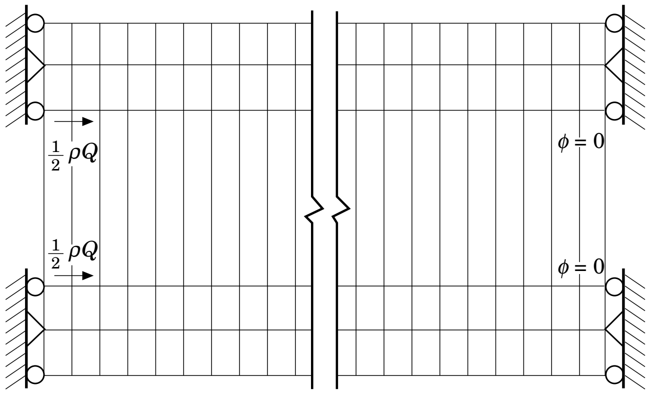

Figure 8. Finite element model for fixed–fixed pipe.

boundary conditions at the inflow and outflow are: at the inlet to the system we specify the gradient of the velocity potential, while at the outflow boundary the velocity potential is fixed at zero (since the pressure is zero there).

Figures 9 and 10 show plots of the mid-span deflection of the pipe versus dimensionless time for zero flow and a dimensionless flow speed $u = 5$, respectively. The zero flow case, of course, simply verifies the response of the system in its first eigenmode and shows that the response is at a single frequency. Using the same initial conditions for the flow case produces a time-response which has several frequency components since those initial conditions now excite several of the flow-modified modes. By performing a DFT analysis of the time response we can identify the important frequencies in the response. Computing results for several different flow velocities allows us to compare the finite element solutions to the analytical solution, as shown in Figure 11. Notice that the finite element results produce a slightly stiff

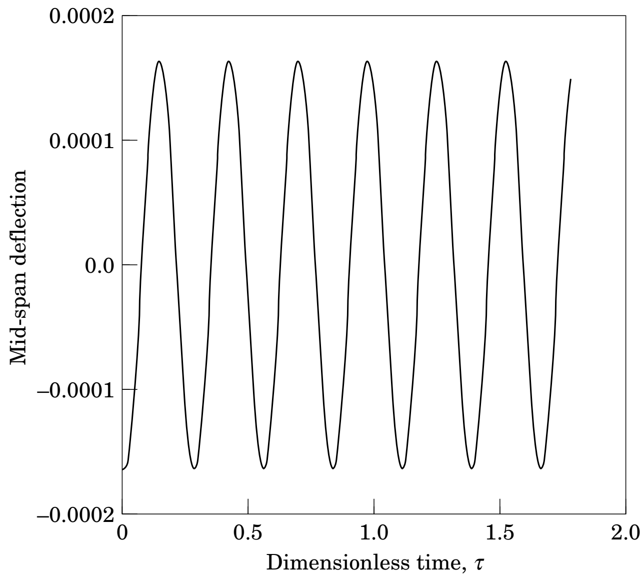

Figure 9. Mid-span deflection of fixed–fixed pipe versus dimensionless time with no fluid flow.

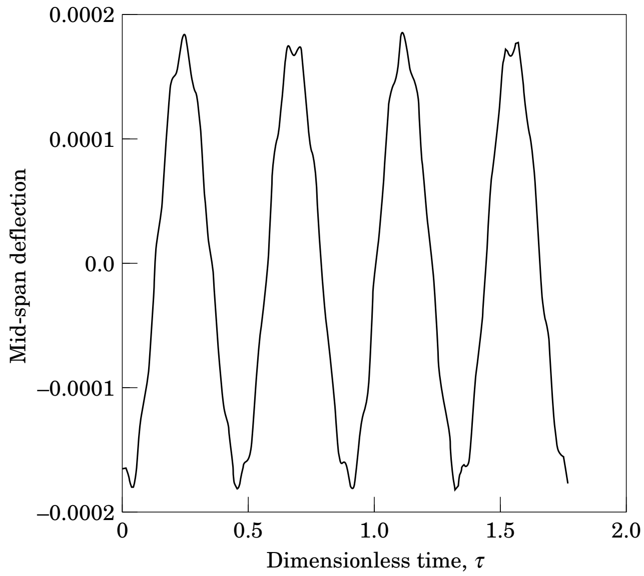

Figure 10. Mid-span deflection of fixed–fixed pipe versus dimensionless time with fluid flow, $u = 5$.

response over the entire flow speed range, as might be expected with four-node solid elements.

3.3. Cantilever Pipe

Figure 12 shows the cantilever pipe studied experimentally and theoretically by Edelstein *et al.* (1986). The behavior of the first mode of the cantilever pipe is very

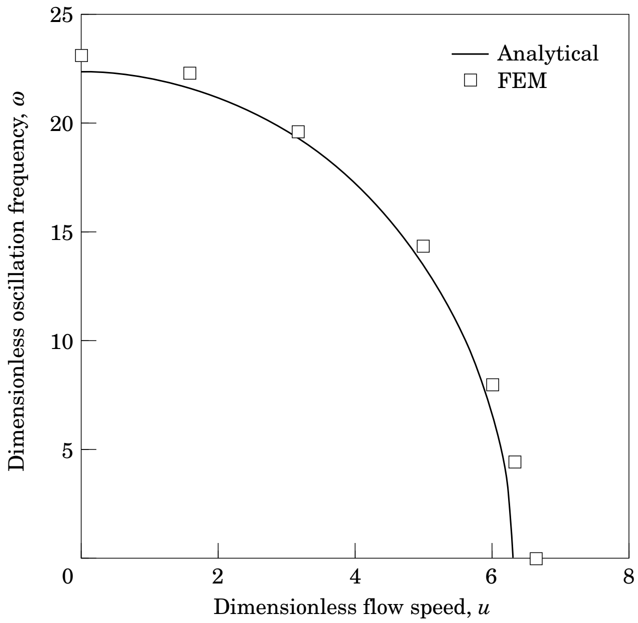

Figure 11. Comparison of finite element and analytical results for frequency versus flow speed for fixed–fixed pipe ($\beta = 0{\cdot}1$).

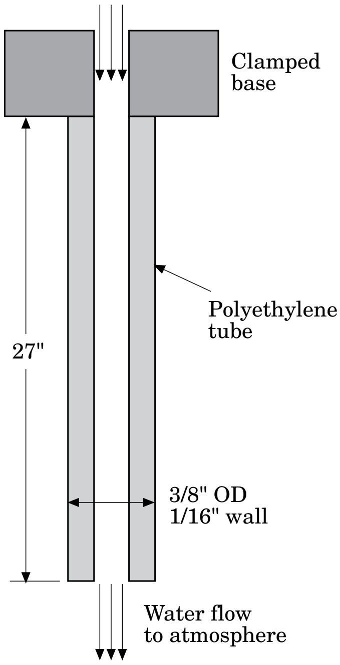

Figure 12. Cantilever pipe ($1'' \equiv 1$ in $= 25{\cdot}4$ mm).

different from that of the fixed-fixed pipe. As Edelstein *et al.* state, "At zero flow, the tube responds as a beam to an initial disturbance. As the flow velocity increases, tube damping values increase.... When the flow velocity is relatively high, the tube is critically damped.... However, when the flow velocity is further increased, damping becomes smaller again, and eventually, the tube loses stability by flutter". By applying the appropriate cantilever boundary conditions to the linearized equation (1) we can once again identify the dominant response modes for a given flow velocity, but the computation is made more difficult by the fact that the characteristic frequencies are complex.

The mesh and boundary conditions for the finite element analysis are shown in Figure 13. The geometry was taken to be the same as in the fixed–fixed pipe, but the solid material properties were changed to simulate the relative mass of $\beta = 0{\cdot}484$ used in the experiment (Young's modulus $6{\cdot}61 \times 10^8$ N/m^2, density 1070 kg/m^3.) The fluid properties were unchanged. Once again a proper imposition of the boundary conditions on the flow is essential for accurate computations. Because the pipe end is moving, we can no longer fix the outflow velocity potential at zero. Therefore, we apply a zero velocity potential as the inflow boundary condition and specify the gradient of the velocity potential at the outflow boundary.

It is important to note that our discrete finite element model should be expected to give good approximations to the true response of the continuous system, since we are examining the response of the lowest mode in a discrete system with almost 2000 degrees of freedom. Thus, we are not likely to observe the discrepancies between discrete and continuous systems that Païdoussis & Deksnis (1970) observed for nonconservative systems when the number of degrees of freedom was small compared to the number of modes examined.

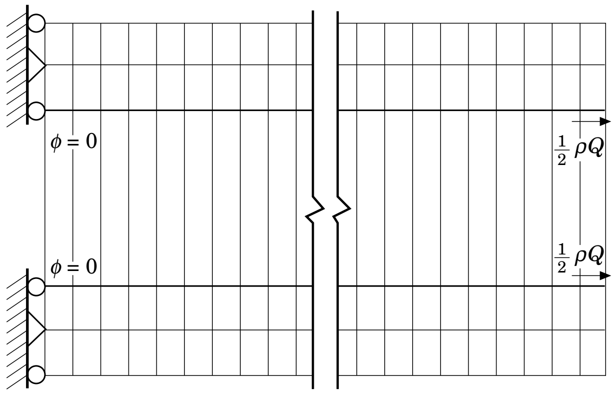

Figure 13. Finite element model for cantilever pipe.

Figures 14 through 17 compare the tip deflection versus time for the finite element solution to the response of the first mode of the system determined from the analytical solution. When the water velocity is 1 m/s (Figure 14), the tube response shows substantial damping. There is good agreement between the finite element solution and the response of the system in its first analytical mode. As the flow velocity is increased to 8 m/s, the tube becomes heavily damped (Figure 15). Here the agreement between the finite element and first mode responses is relatively poor, primarily because several flow-modified modes participate at this flow speed. As the flow velocity is increased to 20 m/s the tube damping again decreases (Figure 16) and the agreement between the finite element and first mode solutions is good. At a flow velocity of 24 m/s the response of the system is clearly unstable, in agreement with the first mode analytical solution (Figure 17). Notice also that the frequency has changed by almost a factor of

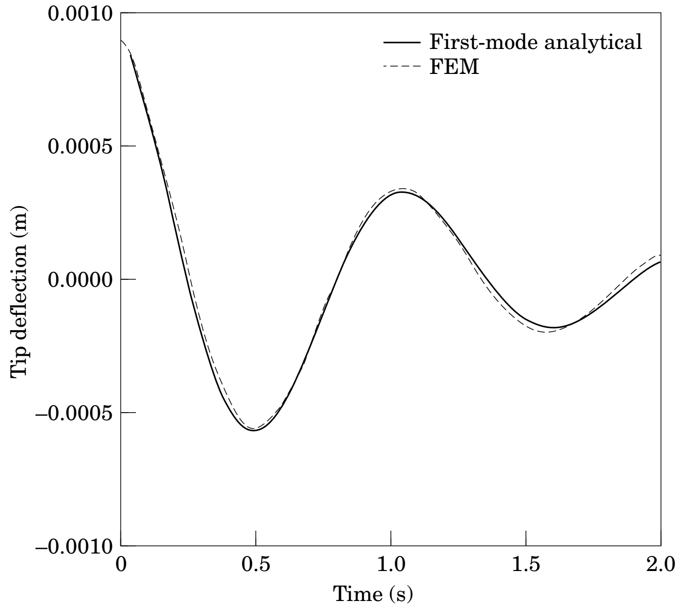

Figure 14. Finite element tip deflection versus time and response of first analytical mode for cantilever pipe. Water velocity 1 m/s, first analytical frequency $\omega = 5{\cdot}7 + 1{\cdot}0i$.

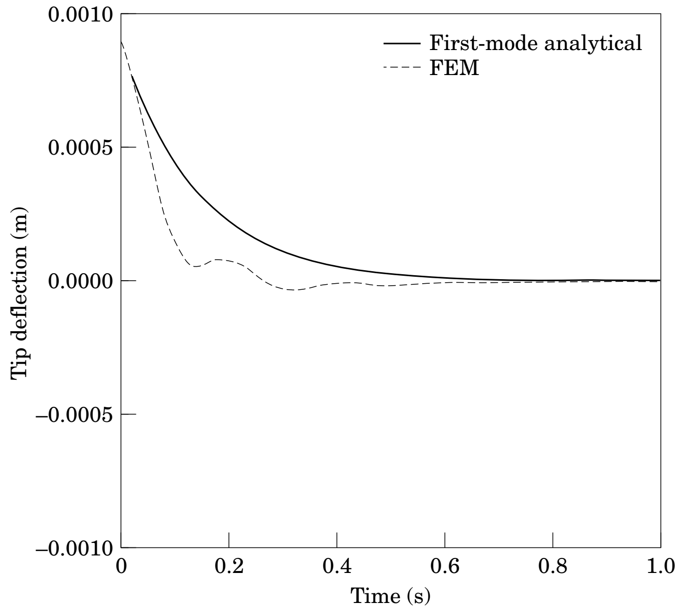

Figure 15. Finite element tip deflection versus time and response of first analytical mode for cantilever pipe. Water velocity 8 m/s, first analytical frequency $\omega = 7{\cdot}0\text{i}$.

ten as the flow speed was increased from 1 to 24 m/s. Despite the rich and complicated nature of the pipe response at various flow speeds, the coupled nonlinear fluid–structure interaction formulation was able to capture the important features of the deflection versus time.

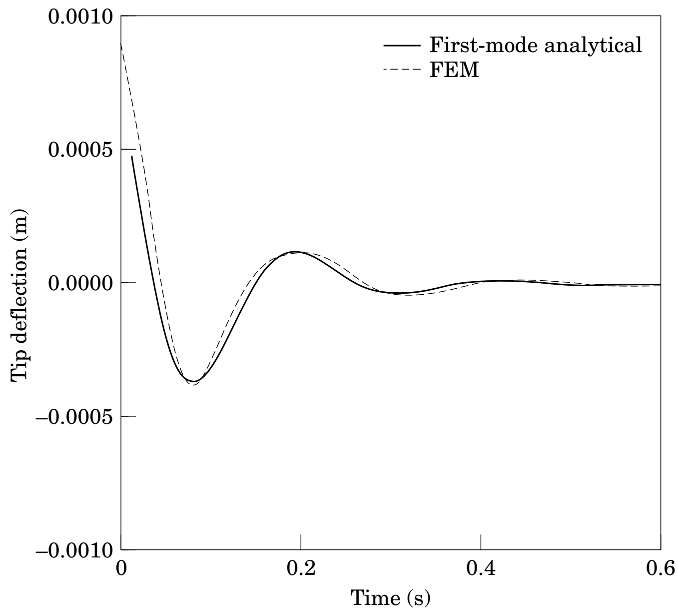

Figure 16. Finite element tip deflection versus time and response of first analytical mode for cantilever pipe. Water velocity 20 m/s, first analytical frequency $\omega = 27{\cdot}8 + 10{\cdot}2\text{i}$.

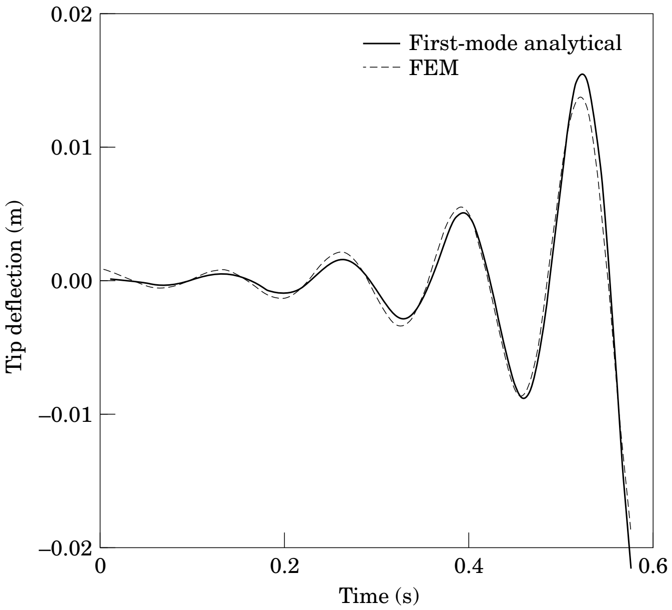

Figure 17. Finite element tip deflection versus time and response of first analytical mode for cantilever pipe. Water velocity 24 m/s, first analytical frequency $\omega = 48{\cdot}4 - 8{\cdot}7\mathrm{i}$.

3.4. Spring-Supported Cantilever Pipe

In order to demonstrate the flexibility of a general purpose finite element code for fluid flow problems, let us modify the properties of the pipe from the previous example so that $\beta = 0{\cdot}2$, and add a spring to restrict the motion of the free end. This is the case discussed by Chen (1987), where he specifically chose $\bar{\alpha} = k_s L^3/EI = 10$. The mesh and boundary conditions are unchanged, except for the addition of the spring.

Figure 18 compares the data from Chen's graph to the finite element results for dimensionless flow velocities from $u = 0$ to $u = 5$, and shows reasonable agreement for the real and imaginary parts of the dimensionless frequency. Notice that the plot compares results for both modes 1 and 2 at dimensionless flow velocities of 4 and 5. Because the method used to excite the transient response of the system uses mode 1 from the zero-flow case, at low flow speeds we observe a transient response dominated by motion in mode 1. As the flow speed increases, the zero-flow mode-1 initial values excite substantial motions in both modes 1 and 2. (In this case, the frequencies can be most easily extracted from the discrete transient response by a least-squares fit of the data.) Once again it is clear that the discrete finite element methods employed here track the transient response of the continuous system well, and that the real and complex parts of the lowest modes of the system may be extracted with reasonable accuracy from the transient data.

4. DISCUSSION AND FUTURE WORK

As has been observed for some time, flow in flexible pipes can drastically alter the oscillation frequencies and transient response of the pipes. In engineering design of piping systems it may be important to account for fluid flow in studying system stability to various loading conditions. Until recently, it was impossible to include fluid flow

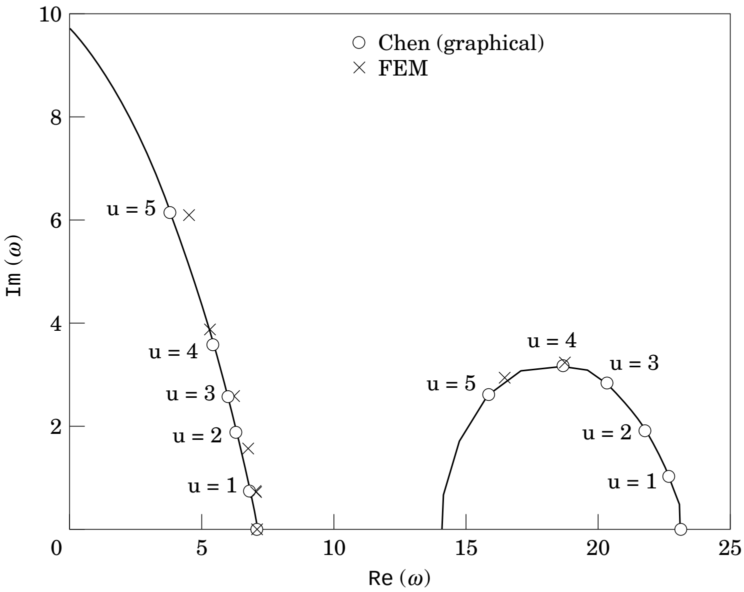

Figure 18. Comparison of finite element and analytical solutions to the spring-supported cantilever pipe test case: the imaginary versus the real component of the dimensionless frequency, $\mathscr{Im}(\omega)$ and $\mathscr{Re}(\omega)$, respectively, for varying u.

effects accurately in the finite element analyses of piping systems which are generally used to assess the system designs.

As we have demonstrated in this study, it is currently possible to use appropriate general purpose finite element programs to predict the response of elastic pipes conveying fluid. The formulation used is nonlinear, employs a Lagrangian–Eulerian approach to allow the fluid to track the solid, and includes bulk flow effects in the fluid. Careful use of such a formulation (in particular, careful attention to the fluid inflow and outflow boundary conditions) gave us good comparisons with analytical solutions for the four test cases examined: a simplified cantilever pipe, a fixed–fixed pipe, a cantilever pipe, and a spring-supported cantilever pipe.

A number of relatively straightforward extensions to the method have not been addressed in this paper, but could be accommodated in future work. In the test cases examined here the solid has been treated as linear elastic and the displacements are small, but the overall coupled fluid–structure problem is treated as nonlinear. If we introduce initial conditions which are not small, the resulting motions of the pipe will be geometrically nonlinear. Alternatively, one could employ a nonlinear material model for the solid and examine the effects of strain-softening or strain-hardening in the pipe material. Contact problems such as the effect on the system of a springy stop on one side could also be included. Nonlinearities which have been studied by other researchers (Païdoussis & Li 1993) could be examined as well. To extend the basic method to three-dimensions requires that a three-dimensional mesh be created and analysed (which would be extremely computer intensive). However, by incorporating shell elements and their associated coupling matrices into the code, a reduction in the three-dimensional analysis time could be effected. Because it is a finite element method, various linear or nonlinear springs could be added, or the geometry of the pipe could be changed so that it is first straight, then slowly tapering, or even curved.

Additional fluid nonlinearities are not as simple to include. The ideal fluid is already nonlinear in the usual finite element sense, since the $\frac{1}{2}\rho V^2$ term is properly accounted for in the fluid equations. Changes in the geometry of the pipe which affect the fluid flow *but which do not impact the ideal fluid assumption* may be included—the pipe can taper, be curved, and so forth. A fluid–velocity dependent friction force at the wall of the pipe could be included. However, incorporating truly viscous effects is not, realistically, an option with the current formulation. Because the fluid formulation is based on a velocity potential, it is not capable of (for example) properly accounting for viscous separation at sudden changes in pipe diameter. To incorporate true viscous action would require a full solution of the (turbulent!) Navier-Stokes equations, coupled with the nonlinear solid motion. Such studies are generally tremendously expensive computationally.

In future work in this area, it would be useful to give special attention to reducing the computational cost of three-dimensional analyses which could more directly simulate actual pipes. Effects on the transient response of engineering piping systems to various practical modifications could then be studied in this manner.

References

Bathe, K. J. 1996 *Finite Element Procedures.* Englewood Cliffs, NJ.: Prentice-Hall.

Benjamin, T. B. 1961 Dynamics of a system of articulated pipes conveying fluid. Part 1. theory. *Proceedings of the Royal Society of London,* Series A **261,** 457–486.

Chen, S. S. 1972a Flow-induced in-plane instabilities of curved pipes. *Nuclear Engineering and Design* **23,** 29–38.

Chen, S. S. 1972b Vibration and stability of a uniformly curved tube conveying fluid. *Journal of the Acoustical Society of America* **51,** 223–232.

Chen, S. S. 1973 Out-of-plane vibration and stability of curved tubes conveying fluid. *Journal of Applied Mechanics* **40,** 362–368.

Chen, S. S. 1987 *Flow-Induced Vibration of Circular Cylindrical Structures.* New York: Hemisphere Publishing Corporation.

Edelstein, W. S., S. S. Chen & J. A. Jendrzejczyk 1986 A finite element computation of the flow-induced oscillations in a cantilevered tube. *Journal of Sound and Vibration* **107,** 121–129.

Hannoyer, M. J. & M. P. Païdoussis 1979 Dynamics of slender tapered beams with internal or external axial flow. Part 2: Experiments. *Journal of Applied Mechanics* **46,** 52–57.

Kock, E. & L. Olson 1991 Fluid-structure interaction analysis by the finite element method. A variational approach. *International Journal for Numerical Methods in Engineering* **31,** 463–491.

McIver, D. B. 1973 Hamilton's principle for systems of changing mass. *Journal of Engineering Mathematics* **7,** 249–261.

Mote, Jr., C. D. 1972 Dynamic stability of axially moving materials. *Shock and Vibration Digest* **4**(4), 2–11.

Nitikitpaiboon, C. & K. J. Bathe 1993 An arbitrary Lagrangian-Eulerian velocity potential formulation for fluid-structure interaction. *Computers and Structures* **47,** 871–891.

Olson, L. G. 1987 Static analysis of contained fluids with potential-based and displacement-based fluid finite elements. *Engineering Computations* **4,** 131–138.

Olson, L. G. & K. J. Bathe 1983 A study of displacement-based fluid finite elements for calculating frequencies of fluid and fluid-structure systems. *Nuclear Engineering and Design* **76,** 137–151.

Olson, L. G. & K. J. Bathe 1985 Analysis of fluid-structure interactions. A direct symmetric coupled formulation based on the fluid velocity potential. *Computers and Structures* **21,** 21–32.

Païdoussis, M. P. 1970 Dynamics of tubular cantilevers conveying fluid. *I. Mech. E. Journal of Mechanical Engineering Science* **12,** 85–103.

Païdoussis, M. P. 1975 Flutter of conservative system of pipes conveying incompressible fluid. *I. Mech. E. Journal of Mechanical Engineering Science* **17,** 19–25.

PAÏDOUSSIS, M. P. 1987 Flow-induced instabilities of cylindrical structures. *Applied Mechanics Reviews* **40,** 163–175.

PAÏDOUSSIS, M. P., J. CUSUMANO & G. COPELAND 1992 Low-dimensional chaos in a flexible tube conveying fluid. *Journal of Applied Mechanics* **59,** 196–205.

PAÏDOUSSIS, M. P. & E. B. DEKSNIS 1970 Articulated models of cantilevers conveying fluid: The study of a paradox. *I. Mech. E. Journal of Mechanical Engineering Science* **12,** 288–300.

PAÏDOUSSIS, M. P. & G. X. LI 1993 Pipes conveying fluid: A model dynamical problem. *Journal of Fluids and Structures* **7,** 137–204.

PAÏDOUSSIS, M. P. & C. SUNDARARAJAN 1975 Parameteric and combination resonances of a pipe conveying pulsating fluid. *Journal of Applied Mechanics* **42,** 780–784.

SÄLLSTRÖM, J. H. 1990 Fluid-conveying damped Rayleigh-Timoshenko beams in transverse vibration analyzed by use of an exact finite element. Part II: Applications. *Journal of Fluids and Structures* **4,** 573–582.

SÄLLSTRÖM, J. H. 1993 Fluid-conveying damped Rayleigh-Timoshenko beams in transient transverse vibration studied by use of complex modal synthesis. *Journal of Fluids and Structures* **7,** 551–563.

SÄLLSTRÖM, J. H. & B. A. ÅKESSON 1990 Fluid-conveying damped Rayleigh-Timoshenko beams in transverse vibration analyzed by use of an exact finite element. Part I: Theory. *Journal of Fluids and Structures* **4,** 561–572.

WICKERT, J. & C. D. MOTE, Jr. 1988 Current research on the vibration and stability of axially-moving materials. *Shock and Vibration Digest* **20**(5), 3–13.